

Case Report

Vascular Findings in the Choriocapillaris in a Case of Radiation Retinopathy Secondary to Choroidal Melanoma

Elaine M. Binkley^{a, b} Lola P. Lozano^{a, b} Megan J. Riker^{a, b}
Edward C. Pennington^c Budd A. Tucker^{a, b} Edwin M. Stone^{a, b}
H. Culver Boldt^{a, b} Robert F. Mullins^{a, b}

^aDepartment of Ophthalmology and Visual Sciences, University of Iowa, Iowa City, IA, USA; ^bInstitute for Vision Research, University of Iowa, Iowa City, IA, USA; ^cDepartment of Radiation Oncology, University of Iowa, Iowa City, IA, USA

Keywords

Choriocapillaris · Choroidal melanoma · Radiation retinopathy

Abstract

The effects of radiation retinopathy on the retinal vasculature have been well established; however, the literature describing the pathologic changes in the choriocapillaris is relatively lacking. In this report, we describe the histologic findings of a donor eye with a choroidal melanoma with special attention to the choriocapillaris. Clinical and histological findings, including immunohistochemistry and transmission electron microscopy, are described for the retina and choroid of a donor eye affected by radiation retinopathy secondary to treatment of choroidal melanoma. Cells within the tumor exhibited an epithelioid structure and balloon melanosomes. Notable infiltration of macrophages with elongated morphology was also observed. Atrophy of photoreceptors, retinal pigmented epithelium, and choriocapillaris was observed on the inferior edge of the lesion and extending past the tumor. The choriocapillaris endothelium showed more severe dropout at the periphery of the lesion where loss of fenestration, thickened cytosol, and degenerated pericytes were observed. Morphologic analysis revealed choriocapillaris loss with pronounced degeneration of choroidal pericytes. Understanding the differences in sensitivity to radiation injury between different cell types and different patients will provide better insight into radiation retinopathy.

© 2022 The Author(s).
Published by S. Karger AG, Basel

Correspondence to:
Elaine M. Binkley, elaine-binkley@uiowa.edu

Introduction

While brachytherapy for uveal melanoma allows for globe salvage in many cases, most patients experience vision loss over time due to sequelae from radiation retinopathy and optic neuropathy. In the Collaborative Ocular Melanoma Study (COMS), 43–49% of patients had vision of 20/200 or worse by 3 years after treatment with brachytherapy [1]. Given that the fundamental reason that many patients elect for brachytherapy as opposed to enucleation is to preserve some useful vision, the mechanisms by which vision loss occur following brachytherapy must be further investigated in order to develop targeted approaches to treatment. Vision loss from radiation retinopathy tends to be delayed and varies considerably from patient to patient. Factors such as tumor size, tumor location, dose to the fovea and optic disc, and comorbid vascular disorders such as diabetes contribute to vision loss, but the precise biologic mechanisms behind the variability from patient to patient are not known [1].

In many cases, both radiation retinopathy and optic neuropathy contribute to vision loss following brachytherapy. Work by Archer and Gardiner described the role of damage to the retinal endothelial cell with relative preservation of the pericyte as part of the proposed mechanism of vascular damage following radiation [2]. While damage to the choroid also occurs following radiation, this has been less well defined and studied. Recent work by Platt et al. [3] examined histopathology from 18 eyes in patients with uveal melanoma who had been enucleated due to sequelae from radiation. They found that 16/18 eyes had some degree of radiation-associated choroidopathy, highlighting the role that the choroid may play in radiation-associated vision loss [3]. We aimed to further examine the radiation-induced ultrastructural changes in the retina and choroid through histopathological, immunohistochemical, and electron microscopy analysis in an eye from an individual treated with plaque brachytherapy for uveal melanoma.

Case Report

A man in his 70s presented for evaluation of a suspicious choroidal lesion in the left eye. He had no prior history of choroidal nevus or other malignancies. His past medical history was significant for type 2 diabetes without retinopathy, hypertension, and hyperlipidemia. Visual acuity was 20/20 in the right eye and 20/25 in the left eye. On exam, in the left eye, in the superotemporal periphery, there was a 14.0 × 9.0 × 3.2 mm dome-shaped choroidal mass with overlying orange pigment. There were no drusen or subretinal fluid over the lesion (Fig. 1). He had no diabetic retinopathy in either eye. Standardized echography showed medium-to-low reflectivity and 1+ vascularity. He was diagnosed with medium-sized choroidal melanoma in the left eye. Following a negative metastatic screening evaluation, he underwent treatment with iodine-125 plaque brachytherapy with a COMS-style plaque. Our institution aims to treat the tumor apex with an 85 Gy dose. In addition to intraoperative ultrasound to confirm plaque placement, we perform postoperative ultrasound on days 1–3 post-plaque insertion. In many cases, there is intra-tumoral edema/hemorrhage or hemorrhage/edema beneath the plaque that can shift the plaque out of the 85-Gy dose range. We therefore add additional thickness to the planned brachytherapy dose in anticipation of tumor edema and/or fluid beneath the plaque. In this case, this resulted in a prescribed dose of 103 Gy to the tumor apex; however, this was closer to 85 Gy of delivered dose given; edema beneath the plaque was noted on the patient's postoperative day #3 echography. Gene expression profile testing at the time of plaque brachytherapy returned a class 2 result.

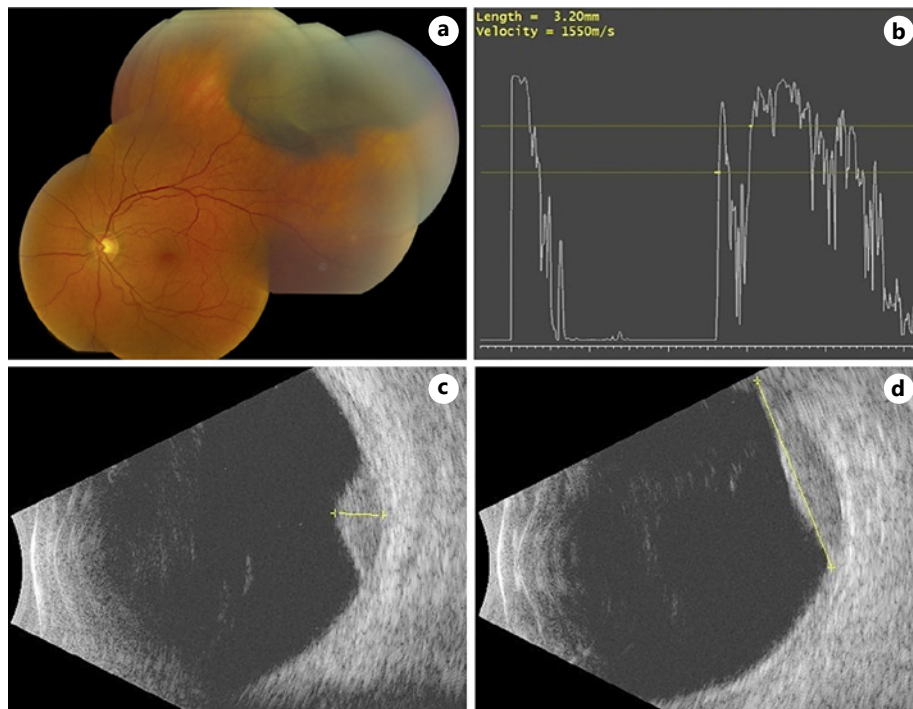


Fig. 1. Images at presentation. Color fundus photography demonstrated a dome-shaped pigmented choroidal lesion located in the superotemporal periphery of the left eye with faint overlying orange pigment (a). Standardized echography showed low-medium reflectivity on the A-scan (b), thickness 3.2 mm on the transverse B-scan (T2E) (c), and 13.5 mm basal dimension on the longitudinal B-scan (L2) (d).

Following brachytherapy, the tumor involuted appropriately. He developed radiation retinopathy with a few cotton wool spots in the superior macula noted 20 months following brachytherapy but initially maintained 20/25 acuity and was observed (Fig. 2). His vision declined to 20/40 with fovea-involving macular edema at the time of his visit 33 months post-brachytherapy, and he began treatment with bevacizumab injections every 4–5 weeks. At the time of his last ophthalmology follow-up 59 months posttreatment, the tumor remained involuted with a decrease in tumor thickness to 1.3 mm (Fig. 3). His acuity had declined to 20/300 in the left eye due to sequelae of radiation, and on exam, he had marked foveal cystoid macular edema, subretinal fluid, and lipid exudates (Fig. 2, 3). He was followed with surveillance imaging of the abdomen every 6 months without evidence of metastatic disease.

Sixty months following plaque brachytherapy, he developed abdominal pain, nausea, and weakness and was found to have biopsy-proven metastatic disease to the liver with hepatic failure. Given the extent of hepatic failure, chemotherapy was deemed to be unhelpful, and he elected to undergo palliative care. He passed away from complications of hepatic failure 62 months following brachytherapy.

The patient donated his eyes for research. Full consent was obtained from the patient's next of kin, and all procedures were in compliance with the Declaration of Helsinki. Posterior poles were preserved by immersion in 4% paraformaldehyde within 6 h of death and were fixed for 2 h, followed by transfer to 10 mM phosphate-buffered saline.

On dissection and gross photomicrography, the superotemporal pigmented lesion was observed (Fig. 4a). Atrophic retinal pigmented epithelial changes were noted, especially temporal to the tumor (Fig. 4a, b). A sagittal section running through the temporal aspect of the lesion to the macula was collected and was infiltrated with graded sucrose solutions and

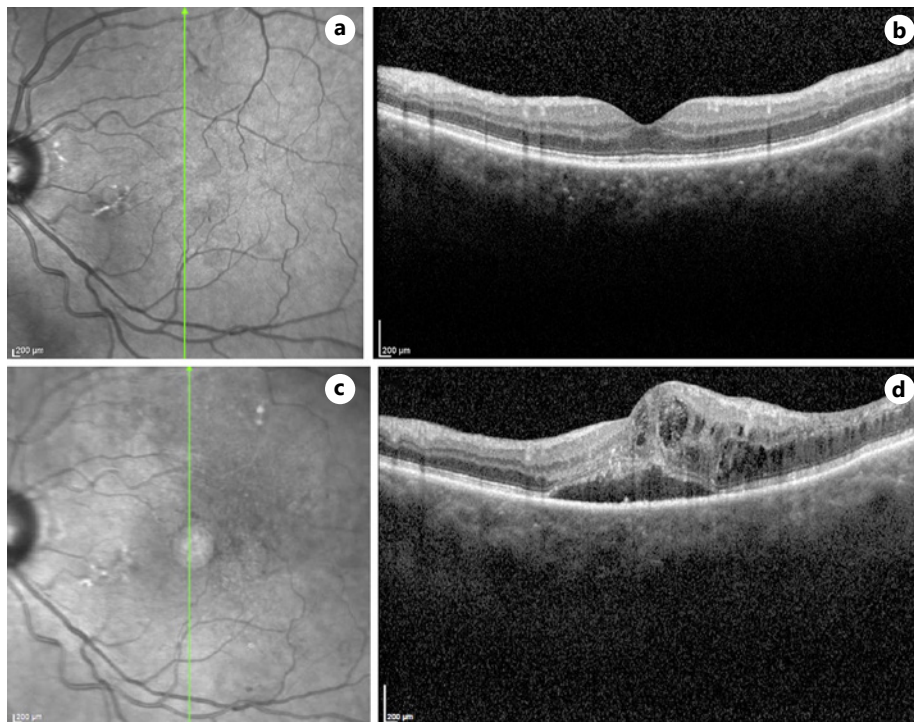


Fig. 2. Optical coherence tomography (OCT) images of the left eye at 20 and 59 months post-brachytherapy. Infrared image at 20 months post-brachytherapy demonstrated lipid exudates and microaneurysms (a). OCT through the fovea showed an absence of cystoid macular edema (b). Infrared image at 59 months post-brachytherapy showed lipid exudates and microaneurysms (c). OCT through the fovea showed marked cystoid macular edema and subretinal fluid (d).

embedded in an optimal cutting temperature compound as described previously [4], and sections were collected along the edge of the rectangle containing the tumor. In addition, a full-thickness 4-mm punch was also collected from within the lesion (Fig. 4b) and fixed in one half strength Karnovsky fixative overnight, followed by osmication, dehydration, embedment in Spurr's resin, sectioning, and imaging on a transmission electron microscope as described previously [5].

Frozen sections were collected and stained with hematoxylin-eosin stain (Fig. 4c) or labeled with the fucose-binding lectin *Ulex europaeus* agglutinin I (UEA-I) and antibodies directed against IBA-1 (Abcam), rhodopsin (Santa Cruz), factor H (Quidel), the C5b-9 membrane attack complex (DAKO), and ICAM1 (Developmental Studies Hybridoma Bank, Iowa City). Sections were viewed on an Olympus BX41 microscope, and digital images collected with a SPOT RT digital camera.

Histopathologic evaluation of the light microscopy wedge revealed that the center of the pigmented lesion, the choroid, was thickened (approximately 365 μm between Bruch's membrane and the inner sclera) with heterogeneous pigmented cells (Fig. 4c). The retinal pigmented epithelium (RPE) was continuous adjacent to the tumor, with notable loss of photoreceptor cells and choriocapillaris extending $\sim 2,050 \mu\text{m}$ past the edge of the tumor toward the macula. Immunohistochemistry was performed, and labeling of the tumor with UEA-I lectin revealed loss of choriocapillaris and depleted intermediate choroidal vessels with relatively poor perfusion throughout the lesion (Fig. 5a–c). Brightfield and IBA-1 immunofluorescence revealed extensive infiltration of macrophages that exhibited an elongated morphology (Fig. 5d, e). In spite of its relatively poor perfusion, the tumor showed considerable

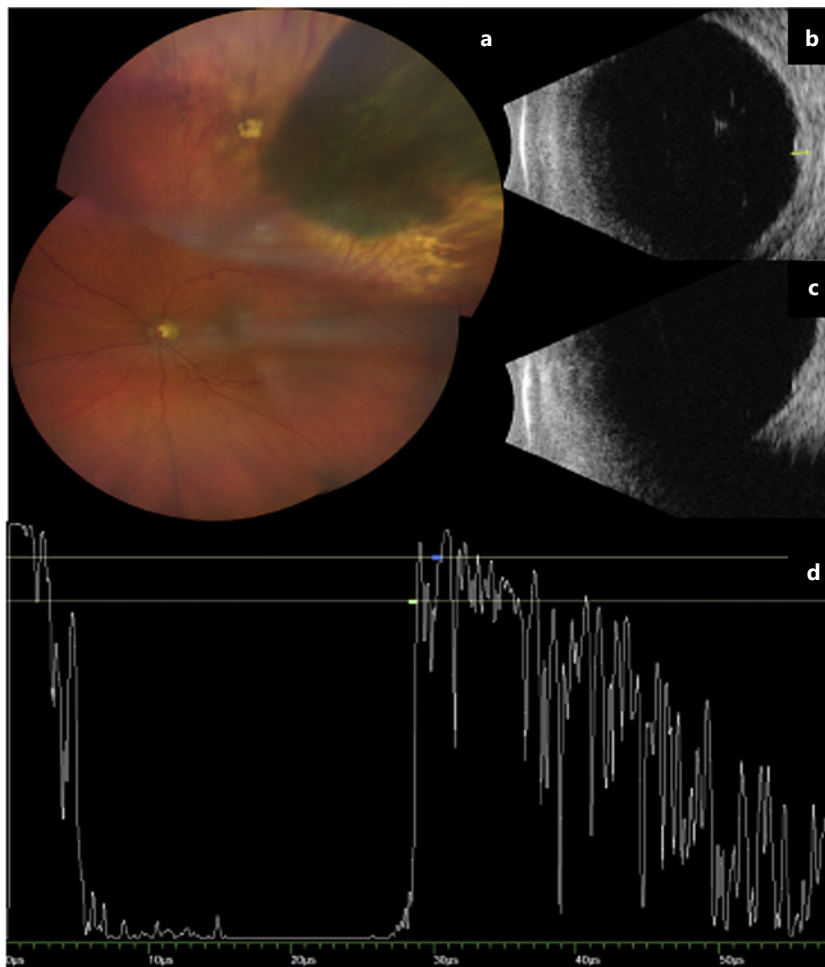


Fig. 3. Images 59 months following brachytherapy. Color fundus photography demonstrated an involuted chorioidal lesion with surrounding retinal pigmented epithelial atrophy in the superotemporal mid-periphery. There were several microaneurysms and dot blot hemorrhages in the macula (a). Standardized echography showed decreased tumor size on the B-scan (T2E) (b), L2 (c), and 1.3 mm thickness on the A-scan with high internal reflectivity (d).

immunoreactivity with antibodies directed against complement factor H (CFH) and, in contrast to the choriocapillaris/Bruch's membrane outside of the lesion, little membrane attack complex deposition (Fig. 5f, g).

Electron microscopy ultrastructural analysis showed further evidence of heterogeneous chorioidal tumor cells. In contrast to normal chorioidal melanocytes, pigmented cells in the lesion were epithelioid in appearance with prominent nucleoli (Fig. 6). Cells with granular, compound, and degenerating balloon melanosomes were also observed within the tumor. The RPE directly overlying the tumor were of mostly normal appearance with basal laminar deposit between the RPE plasma membrane and its basal lamina. The choriocapillaris endothelium directly above the tumor appeared relatively normal, in contrast to histological sections nearer the edge of the tumor. Some capillary segments were attenuated with a thickened cytosol and loss of fenestrations. In addition, vesiculated structures interpreted as degenerated chorioidal pericytes were observed to be associated with some capillaries, adjacent to the endothelium and enclosed within a distinct, persistent basal lamina (Fig. 6).

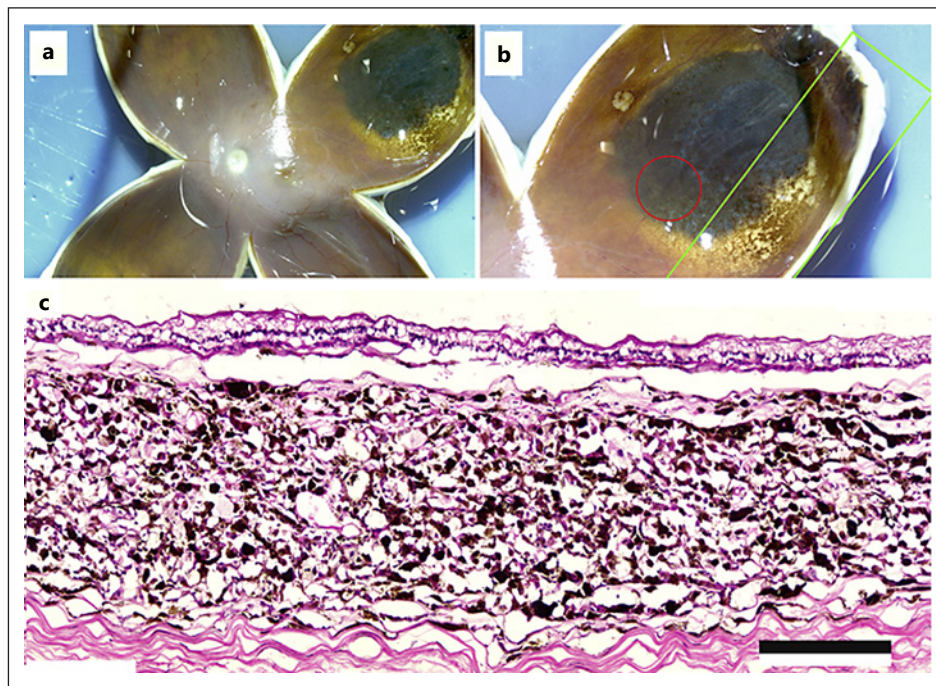


Fig. 4. Gross photograph of donor eye. Note the tumor in the superotemporal choroid and the adjacent atrophy (a). Location of samples collected for light microscopy (green box) and transmission electron microscopy (red circle) (b). Hematoxylin-eosin-stained section of the tumor (c), note the degeneration of the outer retina, RPE, and choriocapillaris. Scale bar, 200 μ m.

Discussion/Conclusion

Here, we describe the ultrastructural changes in an eye with radiation retinopathy following plaque brachytherapy for choroidal melanoma using histopathology, immunohistochemistry, and electron microscopy. We focused on the choriocapillaris given that radiation damage to the choroid has been less well described compared to the retinal vasculature but is an important site of vascular injury in the setting of radiation to the eye [2]. Interestingly, our patient showed relative preservation of the choriocapillaris directly above the tumor but dropout of the choroidal vasculature at the edge of the tumor. This is counterintuitive given that the plaque is placed over the entire surface of the tumor. While a large tumor would result in the plaque being relatively lifted from the choroid, the plaque should still deliver an equivalent radiation dose to the choroid, given the prescribed dose is to the apex of the tumor. Our findings support those of Platt et al. [3] who showed that on histopathologic analysis, in 16 eyes with radiation choroidopathy, 19% had only intra-tumoral choroidal vasculopathy, 19% had only extratumoral radiation choroidal vasculopathy, and 32% had both. The reason for this variation in the distribution of choroidal vasculopathy is uncertain and is an important area for further study. It is possible that the local tumor microenvironment in some cases may result in a protective effect on the overlying vasculature but not in others. Prior work has shown VEGF-A to be increased in eyes with uveal melanoma, with increasing concentrations in tumors with larger basal diameter [6]. It is possible that a pro-angiogenic factor such as VEGF-A may promote maintenance of the choriocapillaris directly above the tumor but not at the edges of the tumor. Variation in tumor size could potentially explain the phenomenon of choriocapillaris loss directly beneath the tumor in some cases but not others. This warrants further quantification of viable choriocapillaris in larger number of patients.

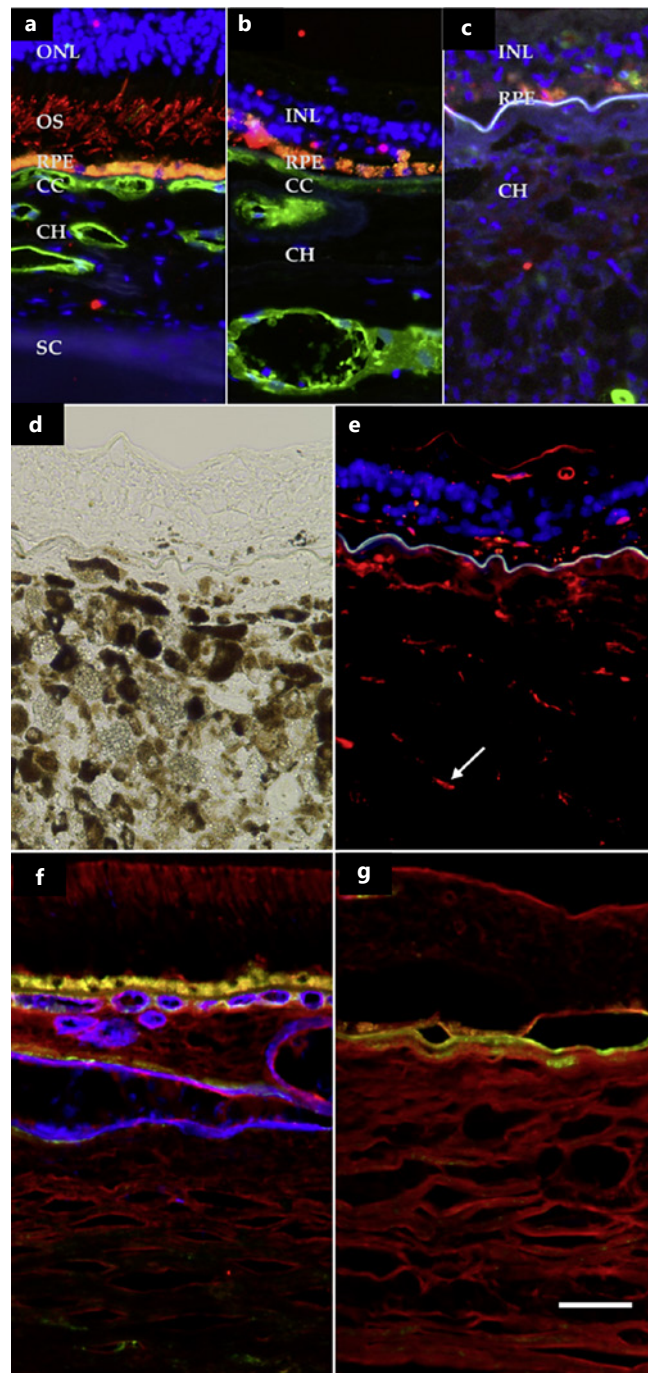


Fig. 5. Fluorescence microscopy of the tumor near the area of atrophy and adjacent choroid. Labeling with the endothelial binding lectin UEA-I (green) and anti-rhodopsin (red) shows relatively normal retina posterior to the tumor (a), transition with loss of choriocapillaris and photoreceptors (b), and over the tumor with sparse viable vasculature, overlying loss of RPE autofluorescence, and loss of the outer nuclear layer (ONL) (c). Bright-field (d) and fluorescence (e) image of the tumor and overlying retina show tumor infiltration by macrophages. e Depicts labeling with the anti-IBA antibody, showing numerous ramified macrophages in the tumor (arrow). Labeling outside the tumor (f) and within the tumor (g) with antibodies directed against CFH (red), the C5b-9 membrane attack complex (green), and UEA-I lectin (blue). Note the strong CFH labeling of the tumor in G despite the lack of vascular elements, suggesting robust local synthesis. INL, inner nuclear layer; OS, photoreceptor outer segments; CC, choriocapillaris; CH, outer choroid; SC, sclera. Scale bar, 50 μ m.

In contrast to prior work by Archer et al. [2] who found a predilection for damage to the endothelial cells rather than the pericytes in the retinal vasculature following radiation, we found greater loss of pericytes relative to endothelial cells at the level of the choroid. While the endothelial cell may be the primary site of damage in some cases, work by Lee et al. [7] showed greater loss of pericytes compared to endothelial cells in areas of radiation necrosis in patients with glioblastoma treated with external beam radiation, suggesting that in some types of radiation damage, the pericyte is a key site of injury. While our patient did have type 2 diabetes that would typically be expected to result in predominantly pericyte rather than

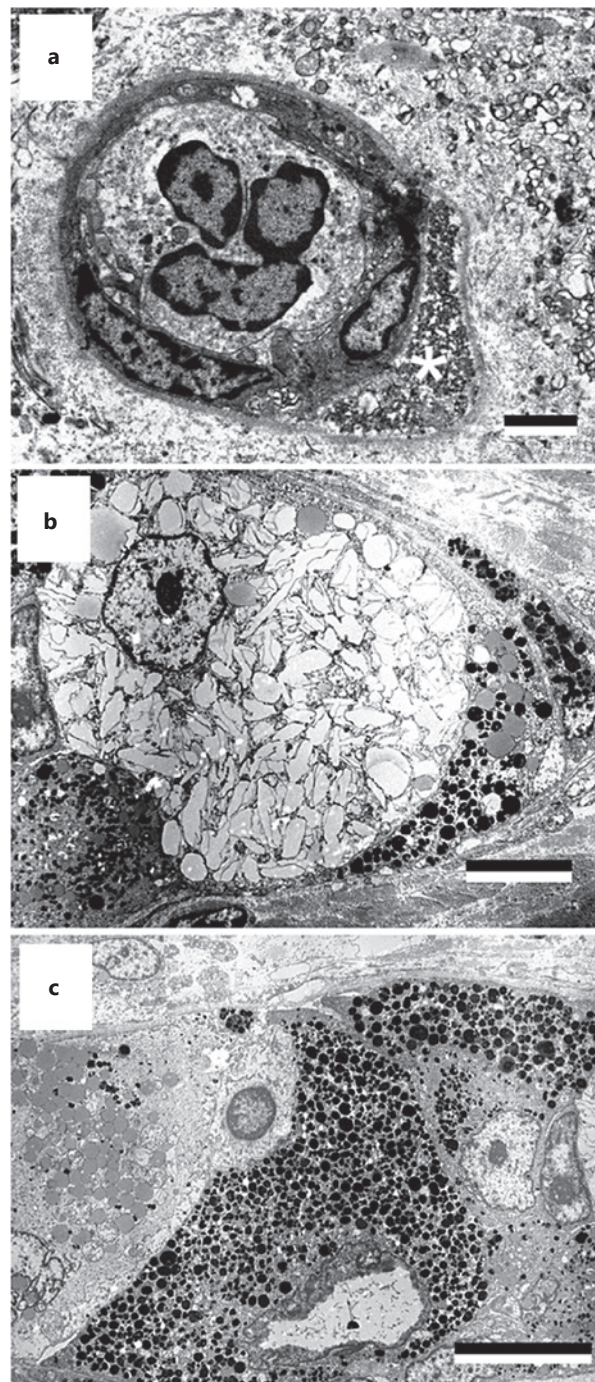


Fig. 6. Ultrastructural findings of the tumor and overlying choriocapillaris. **a** Choriocapillaris vessel with adhered polymorphonuclear phagocyte. The endothelium is attenuated and lacks fenestrae, and the basal lamina extends around an accumulation of debris, presumably the former location of a pericyte (asterisk). The tumor exhibits heterogeneity that includes cells with balloon melanosomes (**b**) and epithelioid cell with prominent nucleoli and heterogeneous pigment, including both granular and compound melanosomes (**c**). Scale bars, 2.5 μm (**a**), 10 μm (**b**), and 12.5 μm (**c**).

endothelial cell loss (at least in the neural retina), he had no diabetic retinopathy in the contralateral eye, suggesting that the microvascular changes in the treated eye were largely due to radiation-related sequelae rather than diabetic retinopathy. It is possible that the cell of primary injury differs in the choroid relative to the retinal vasculature, and this is again an important area of further study as potential novel therapies to reduce the risk for radiation-related vision loss would need to be targeted accordingly.

We observed robust labeling of the tumor in our patient with antibodies directed against CFH, a soluble inhibitor of the alternative complement cascade. Through its interactions with

CFI and C3b, CFH prevents formation of the membrane attack complex and complement-mediated cell lysis. As an immune evasion strategy, various cancers have been found to express CFH. While the literature regarding expression of CFH in uveal melanoma is lacking, uveal melanoma cells upregulate expression of CD47, PD-L1, MHC molecules, and IDO-1 [8]. In other cell types, IDO-1 inhibition is related to decreased expression of CFH, whereas TNF- α and IFN- γ (both elevated in the vitreous of melanoma patients) increase CFH expression [9, 10]. The altered expression of IDO-1, TNF- α , and IFN- γ plausibly plays a role in the observed CFH expression and immune evasion by uveal melanoma.

We show that in an eye treated with plaque brachytherapy for choroidal melanoma, the choriocapillaris directly beneath the plaque was relatively preserved compared to the edges of the tumor and that the pericyte was the primary site of injury in the choroid. These are important findings that require further study in an effort to better understand and design novel therapies to reduce the risk of vision loss following brachytherapy for uveal melanoma.

Acknowledgments

The authors would like to acknowledge Mrs. Connie Hinz.

Statement of Ethics

Ethical approval was not required in accordance with our institutional guidelines as this patient is deceased. This case was reviewed by the decedent board at the University of Iowa and was given consent for publication. Full consent was also obtained from the patient's next of kin, and all procedures were in compliance with the Declaration of Helsinki. Written informed consent was obtained from the patient's next of kin for publication of the details of their medical case and any accompanying images.

Conflict of Interest Statement

The authors have no conflicts of interest to declare.

Funding Sources

Supported in part by NIH P30 EY025580. The funders had no role in study design, data collection and analysis, decision to publish, or preparation of the manuscript.

Author Contributions

Design of work: Elaine M. Binkley, Edward C. Pennington, H. Culver Boldt, and Robert F. Mullins; data acquisition, interpretation, and analysis: Elaine M. Binkley, H. Culver Boldt, Lola P. Lozano, Edward C. Pennington, Robert F. Mullins, Megan J. Riker, and Budd A. Tucker; drafting and critically revising work: Elaine M. Binkley, H. Culver Boldt, Lola P. Lozano, Robert F. Mullins, Edwin M. Stone, and Budd A. Tucker; final approval: Elaine M. Binkley, H. Culver Boldt, Lola P. Lozano, Edward C. Pennington, Robert F. Mullins, Megan J. Riker, Edwin M. Stone, and Budd A. Tucker.

Data Availability Statement

All data generated or analyzed during this study are included in this article. Further inquiries can be directed to the corresponding author.

References

- 1 Melia BM, Abramson DH, Albert DM, Boldt HC, Earle JD, Hanson WF, et al. Collaborative ocular melanoma study (COMS) randomized trial of I-125 brachytherapy for medium choroidal melanoma. I. Visual acuity after 3 years COMS report no. 16. *Ophthalmology*. 2001;108(2):348–66.
- 2 Archer DB, Amoaku WM, Gardiner TA. Radiation retinopathy – clinical, histopathological, ultrastructural and experimental correlations. *Eye*. 1991;5(Pt 2):239–51.
- 3 Platt S, Salomao DR, Pulido J. Histologic findings of choroidal vasculopathy in eyes enucleated following radiation therapy for uveal melanoma: radiation choroidopathy. *Klin Monbl Augenheilkd*. 2021;238(5):584–90.
- 4 Barthel LK, Raymond PA. Improved method for obtaining 3-microns cryosections for immunocytochemistry. *J Histochem Cytochem*. 1990;38(9):1383–8.
- 5 Schubert C, Pryds A, Zeng S, Xie Y, Freund KB, Spaide RF, et al. Cadherin 5 is regulated by corticosteroids and associated with central serous chorioretinopathy. *Hum Mutat*. 2014;35(7):859–67.
- 6 Missotten GSO, Notting IC, Schlingemann RO, Zijlmans HJ, Lau C, Eilers PHC, et al. Vascular endothelial growth factor a in eyes with uveal melanoma. *Arch Ophthalmol*. 2006;124(10):1428–34.
- 7 Lee ST, Seo Y, Bae JY, Chu K, Kim JW, Choi SH, et al. Loss of pericytes in radiation necrosis after glioblastoma treatments. *Mol Neurobiol*. 2018;55(6):4918–26.
- 8 Basile MS, Mazzon E, Fagone P, Longo A, Russo A, Fallico M, et al. Immunobiology of uveal melanoma: state of the art and therapeutic targets. *Front Oncol*. 2019;9:1145.
- 9 Tu Z, Li Q, Bu H, Lin F. Mesenchymal stem cells inhibit complement activation by secreting factor H. *Stem Cells Dev*. 2010;19(11):1803–9.
- 10 Nagarkatti-Gude N, Bronkhorst IHG, van Duinen SG, Luyten GPM, Jager MJ. Cytokines and chemokines in the vitreous fluid of eyes with uveal melanoma. *Invest Ophthalmol Vis Sci*. 2012;53(11):6748–55.